Main Manuscript for

Local alkalinity enhancement using artificial substrates increases survivorship of early-stage coral recruits

Melissa Ruszczyk[1, **], Skylar Rodriguez[2, **], Montale Tuen[3], Kylee Rux[3], Santhan Chandragiri[1], Maren Stickley[2], Brian K. Haus[4], Andrew C. Baker[2], Margaret W. Miller[5], Prannoy Suraneni[3], Chris Langdon[2, *], Vivek N. Prakash[1, 2, 6, *]

[1]Department of Physics, College of Arts & Sciences, University of Miami, Coral Gables, FL
[2]Department of Marine Biology and Ecology, Rosenstiel School of Marine, Atmospheric and Earth Science, University of Miami, Miami, FL
[3]Department of Civil and Architectural Engineering, College of Engineering, University of Miami, Coral Gables, FL
[4]Department of Ocean Sciences, Rosenstiel School of Marine, Atmospheric and Earth Science, University of Miami, Miami, FL
[5]SECORE International, Miami, FL
[6]Department of Biology, College of Arts & Sciences, University of Miami, Coral Gables, FL

**Equal contribution
*Corresponding authors: Chris Langdon, Vivek N. Prakash

Email: clangdon@earth.miami.edu, vprakash@miami.edu

Author Contributions:
Conceptualization: A.C.B., M.W.M., P.S., C.L., V.N.P.
Methodology – AE cement tile design, fabrication: M.T., K.R.
Methodology – topography experiments: M.R.
Methodology – chemistry experiments: M.R.
Methodology – biology experiments: S.R., M.S., M.R.
Data Analysis: M.R., S.R., S.C., C.L., M.W.M., A.C.B.
Writing – original draft: M.R., S.R.
Writing – review, editing: M.R., K.R., M.T., A.C.B., M.W.M., P.S., C.L., V.N.P.
Supervision: A.C.B., M.W.M., P.S., C.L., V.N.P.
Project Administration: B.K.H., A.C.B., M.W.M., P.S., C.L., V.N.P.
Funding Acquisition: A.C.B., C.L., V.N.P.

Competing Interest Statement: The authors do not have any competing interests

Classification: Biological Sciences – Applied Biological Sciences, Physical Sciences – Applied Physical Sciences

Keywords: Alkalinity enhancement, coral, restoration, substrate-sea interface, laminar flows

This PDF file includes:
Main Text
Figures 1 to 4
Table 1

Abstract

Efforts to restore coral reefs using sexually derived coral recruits are often hindered by their low survivorship and growth, hence scalable interventions to improve these parameters are urgently needed. Here we developed novel settlement substrates that modify the local chemical and hydrodynamic environments and provide local alkalinity enhancement (AE) within the laminar boundary layer to aid in coral restoration. Cement tiles with four different chemistries and two different surface topographies were tested in a novel flume system to quantify their ability to change local pH under reef-like conditions and their effect on larval settlement, survivorship, and growth of the endangered Caribbean coral, *Orbicella faveolata*. Chemistry had a minimal effect on the initial settlement of coral larvae, with textured tiles preferred over smooth tiles. However, substrates that created a more alkaline local environment increased post-settlement survivorship. The increased survivorship of *O. faveolata* recruits on AE tiles was not due to increased growth on AE tiles, although trends in growth were dependent on chemistry and topography of tiles. Our results indicate that mixing sodium bicarbonate into the cement used to fabricate artificial reef structures could be an effective means to enhance the development of coral cover.

Significance Statement

Reef-building coral populations in South Florida and the Caribbean are nearing crisis, with low survivorship rates of new recruits being identified as a critical bottleneck limiting their recovery. Although the causes are unknown, slow growth and prolonged vulnerability to predation may play a role. Since ocean acidification is known to stress corals and hinder their growth, we hypothesized that enhancing alkalinity could help mitigate ocean acidification effects. This could also help boost coral growth and increase survivorship during their critical early days. This hypothesis was experimentally tested by adding sodium bicarbonate to settlement substrates, and studying coral spat growth and survival. Our results showed significantly higher survivorship on alkalinity enhanced substrates, indicating that this could be a promising restoration intervention.

Main Text

Introduction

Coastal cities are susceptible to the impacts of waves, flooding, storm surge, and sea-level rise. In response to these threats, coastal jurisdictions invest in engineered shoreline defenses such as breakwaters and seawalls that are expensive to build and maintain. There is growing recognition that approaches which incorporate some features of natural ecosystems, such as coral reefs, could be effective and cost-efficient alternatives. This thinking has given rise to the concept of hybrid structures made of an eco-friendly concrete base with corals attached on top or encouraged to attach naturally. Such reef-mimicking hybrid reefs with an overlay of living corals could offer the immediate benefits of wave attenuation while providing ecosystem benefits and promoting ecosystem resilience (Guannel et al. 2016).

While the concept of hybrid coral reefs sounds attractive, we are amidst a critical time when coral reefs around the world are diminishing. According to the latest status of the world's coral reef report, between 2009 and 2018, there was a progressive loss of about 14% of the coral from the world's coral reefs (Souter et al. 2021). This was primarily due to recurring large-scale

coral bleaching events, combined with other local pressures such as coastal development, land-based and marine pollution, unsustainable fishing, disease, and tropical storms.

The global decline in coral populations creates the snowballing problem of decreased larval supply and decreased genetic diversity of those larvae inhibiting recovery following disturbance. Larval availability, settlement success, and post-settlement survivorship and growth have long been recognized as key factors driving the recovery of coral reefs following disturbances (Hughes et al. 1999). Studies have shown that settlement rates of corals in the Caribbean are much lower than on reefs in the Pacific and Indian oceans (Wilson and Harrison 2005). This could be related to generally much lower coral cover on Caribbean reefs and hence a smaller supply of larvae (Humanes and Bastidas 2015). Slow, early post-settlement growth is an important contributing factor as the slower the growth, the longer the baby corals are in the very small size class that is most vulnerable to predation and competitive exclusion by macro-algae.

Ocean acidification is known to stress corals causing them to grow more slowly or divert energy from other essential life processes to keep up a constant growth rate. This led us to hypothesize that alkalinity enhancement (AE) might be a way to give coral spat a respite from ocean acidification and may be even a boost in their growth that would help relieve the bottleneck and increase survivorship during the critical early days of their lives. Here we describe the results of experiments testing whether AE via substrate is a practical means of improving early post-settlement growth and survival (**Figure 1**). Increasing the alkalinity or saturation state of seawater by the addition of sodium hydroxide, sodium bicarbonate, sodium carbonate, or calcium chloride have been shown to increase calcification of adult corals (Langdon et al. 2000, Herfort et al. 2008, Albright et al. 2016). These studies involved adding chemicals to seawater. While the additions had the desired effect it is unlikely this method would work at scale because of the huge amounts of chemicals that would need to be added given the large volume of seawater that flows over a coral reef every day. Alternatively, compounds increasing alkalinity can be added to substrate and leached into the water column, providing an alkalinity-enhanced environment to settle coral spat (**Figure 1a**). We designed AE tiles made with four different chemistries (Portland limestone cement with no additions, 1% sodium bicarbonate by weight, 1% sodium carbonate by weight, and 2% sodium carbonate by weight) and two different surface topographies (a flat tile, and a tile textured with concave divots) as substrates. These AE tiles may increase local alkalinity in the fluid above both by diffusion and advection inside a boundary layer in the laminar flows generated using a novel flume **(Figure 1b-d)** (Ruszczyk et al. preprint). Carbonate and bicarbonate ions leaching out of the tiles may be sufficient to stimulate early growth of the coral spat through either direct contact of the coral on the substrate or while the coral was small enough to occupy the laminar boundary layer (**Figure 1a**). This AE method via substrates could be easily applied at scale by mixing small amounts of sodium carbonate/bicarbonate into the cement used to fabricate artificial or hybrid reefs.

Results

Tile Verification: Diffusion and Advection

Adding 1-2% sodium bicarbonate or sodium carbonate by weight to cement tiles was sufficient to elevate pH by 0.2 – 0.4 pH units under stagnant flow conditions ($P < 0.0001$) and 0.1 pH units within the laminar boundary layer generated in our flumes (Ruszczyk et al. preprint). The laminar flows in the flumes were comparable to that encountered on a coral reef ($P < 0.0001$, **Figure 2a-c**). Within the laminar boundary layer, all AE tiles significantly increased pH, however, the effect of 2% carbonate tiles in flow was greatly diminished compared to a diffusive setting (**Figure 2c, Supplementary Table S1**). The smaller increase of pH in the advection setting

occurred because the carbonate and bicarbonate leaching out of the cement was diluted by seawater.

Longevity of Tiles

Linear regressions were fitted to the change in pH for the different chemistries versus tile age for measurements at the surface of the tile and 3.26 $\pm$ 0.09 mm above the surface of the tile to capture changes above the surface of the tile and within the laminar boundary layer (**Figure 2d**). There was one outlier in the entire dataset noted for 2% carbonate additions that occurred on day 1 and was excluded from the analysis (but included in **Figure 2d** for reference). Three out of the eight total regressions were significant, indicating the declining effectiveness of tiles with no additions ($P_{Surface}$ = 0.01), and 2% carbonate additions ($P_{Surface}$ < 0.01, P_{Above} = 0.03) to increase pH over the 84 d experiment while 1% bicarbonate addition and 1% carbonate additions did not change with respect to time (**Figure 2d, Supplementary Table S2**).

Data points were grouped by chemistry and measurement location across the 84 d to identify broad trends. At the surface of the tile, 1% bicarbonate additions and 1% carbonate additions increased the pH the most (**Supplementary Table S3**). Additionally, students' t-tests were run to see if the lower performing tiles (i.e., no additions or 2% carbonate additions) still increased pH from 0. All tiles except for those with no additions had an average change in pH greater than zero at the surface of the tile and within the laminar boundary layer (**Supplementary Table S3**) (**Figure 2e**). Overall, these aging tests showed that the AE tiles could elevate pH within the fluid boundary later by 0.05-0.06 units for at least 84 days.

Chemistry and Topography

The chosen tile topographies in this experiment were a flat surface (i.e., a "flat" tile), and a surface textured with divots (i.e., a "textured" tile). There were minimal differences in the flow above the tiles between these two surface topographies with regards to velocity and vorticity, indicating that there is no breakdown of the laminar boundary layer resulting from the tile divots (**Figure S5**). This was because the smooth, laminar flow within the flumes did not generate recirculation regions.

Even though there was no difference in the hydrodynamic environment between the two topographies, the chemical landscape about the tiles differed. A full factorial ANOVA comparing the change in pH with respect to the four different chemistries and two locations within textured tiles (i.e., in a divot or on the surface of the tile) indicated significant differences in ΔpH with respect to chemistry (P < 0.0001) and location (P < 0.0001), with ΔpH being significantly higher in the divots than on the surface of a textured tiles for all chemistries (**Figure 2f-g**). Because there was minimal flow into the divots resulting in minimal advection, the pH in the divots was significantly higher than at the surface. Hence, the divots provide a region sheltered from flow ($u \approx 0$ m s^{-1}).

Settlement

To identify any settlement preference, the number of *O. faveolata* settlers per tile was analyzed on day 0 using an ANOVA with chemistry and topography as factors. There was no significant difference in settlement based on chemistry (P = 0.47), however, textured tiles had higher settlement numbers than flat tiles (P < 0.001, **Figure 3a**). On textured tiles, where corals

had the option of settling on the surface or in a divot, corals preferred settling in divots ($P < 0.01$, **Figure 3b**).

Survivorship

Total survivorship was analyzed using an ANOVA with chemistry and topography as factors at the end of the experiment (139 d), and both chemistry ($P = 0.03$) and tile topography ($P < 0.01$) affected survivorship (**Figure 3c**). Overall, the 1% and 2% carbonate additions showed a clear increase in survivorship (**Figure 3c, d**). Across all 15 tiles, the survivorship on flat surfaces was the same across chemistries and topographies ($P = 0.22$), and the survivorship in divots was the same across the 6 textured tiles ($P = 0.68$) (**Figure 3e**). When comparing the location survivorship (survivorship of surface settlers compared to divot settlers for each tile) on textured tiles, the survivorship of corals settled in divots was significantly lower than the survivorship of corals settled on the surface of tiles ($P < 0.01$) (**Figure 3f-g**).

Growth

Surface area, vertical height, and volume of *O. faveolata* varied with respect to chemistry and topography. Additionally, *O. faveolata* surface area and volume were better predicted when including an interactive effect of chemistry and topography in their respective models (**Supplementary Table S5, Table 1, Figure 4**). Both chemistry and topography were found to be significant predictors when generating GLMs of coral growth data with respect to surface area, skeletal height, and volumetric growth. While none of the chemistries tested is an apparent best choice resulting in the greatest growth – each chemistry has its own growth patterns – topography has a more apparent effect. *Orbicella faveolata* on the surface of textured tiles have a smaller areal size than on the surface of flat tiles. One potential explanation for the lesser growth on textured tiles is that coral growing in divots may have less growth due to competition from other corals and/or algae in a confined space or were spatially limited in the area to which they can grow. However, these individuals were excluded from the growth analysis to maintain consistency with vertical measurement practices, which could not measure the skeletal height of corals grown in divots.

Discussion

Physicochemical Environment of AE Tiles

Adding just 1% to 2% sodium carbonate or bicarbonate by weight to cement tiles was sufficient to elevate the pH in the boundary layer by 0.2-0.4 pH units under stagnant flow. When flow is introduced, 1% carbonate and 1% bicarbonate tiles yield the largest increase in pH (0.1 units) across all chemistries (**Figure 2**)**.** This smaller increase of pH in the advection setting compared to diffusive setting for all chemistries is expected because the carbonate and bicarbonate leaching out of the cement will be diluted by the much larger pool of carbonate and bicarbonate ions in the total seawater. The 2% carbonate tiles have a significantly less impact on local pH in flow conditions compared to diffusive conditions in both the advection verification and in the aging experiments **(Figure 2).**

The reduced effect of 2% carbonate addition tiles on pH in the flow compared to diffusion is unexpected. However, the similar ΔpH values for 2% carbonate on the surface and above the surface indicate a more uniform chemical environment above the tile. This becomes apparent when estimating the Péclet number (Pe) for carbonate ions in this environment. Pe represents the ratio of the advective transport rate to the diffusive transport rate of a substance and is calculated as

$$Pe = \frac{uL}{D} \tag{1}$$

where u represents the flow speed (0.012 m s^{-1}), L is the characteristic length scale (0.03 m, the length of the flume), and D is the diffusion coefficient for a given substance, which can be estimated as

$$D = \frac{k_B T}{6\pi\mu r_i} \quad (2)$$

where k_B is the Boltzman constant (1.38 x 10^{-23} J K^{-1}), T is the absolute temperature of the system (293 K), μ is the dynamic viscosity (8.9 x 10^{-4} Pa s), and r_i is the radius of ion in question. When Pe < 1, diffusion dominates transport, when Pe = 1, advection and diffusion are of equal importance, and when Pe > 1, advection dominates transport (Munson et al. 2013). Here, the Pe for carbonate (r_i = 178 pm) and bicarbonate (r_i = 156 pm) are both much greater than 1 ($Pe_{Carbonate}$ = 2.0 x 10^5, $Pe_{Bicarbonate}$ = 2.3 x 10^5), indicating that advection is more dominant than diffusion within the boundary layer. This is observed in the significantly less intense effect that tiles have on pH when in advective conditions compared to diffusive conditions.

Advection influencing the tile's ability to affect pH also can explain why 2% carbonate addition tiles do not perform as well as 1% bicarbonate and 1% carbonate tiles in flow conditions. The change in pH of 2% carbonate tiles in the aging experiment at the surface were not different than the change in pH above the boundary layer. However, 2% carbonate addition tiles significantly raise the pH above ambient conditions. One possible explanation for this observation is that the 2% carbonate addition tiles leached their carbonate ions into the environment at a rate where advective mixing no longer stratifies the pH below and above the boundary layer, as it did for the 1% bicarbonate and 1% carbonate addition tiles.

Coral response to AE Tiles

Initial settlement of *O. faveolata* was not strongly affected by chemistry; however, settlement was affected by topography. *Orbicella faveolata* prefer settling on textured tiles rather than flat tiles, and within textured tiles, a strong preference to settle within the confines of a divot rather than on the surface (**Figure 3**). Coral recruits are more likely to settle in topographical features close to their size to maximize their area for attachment, a phenomenon coined "attachment point theory" (Whalan et al. 2015, Levenstein et al. 2022). In this experiment, the 3 mm diameter of the divot was approximately six times the diameter of recruits, which provides more surface area as the coral settler can attach to the divot bottom or the wall.

Although *O. faveolata* preferred settling on textured tiles, and specifically, within the divots, *O. faveolata* suffered from higher mortality rates on textured tiles, particularly those that settled in divots, than flat tiles even with AE additions. It is possible the divots were too sheltered from the surrounding environment. Minimal flow was measured in the divots, creating relatively static flow conditions. With no flow to account for advective processes, Pe << 1, so diffusion dominates the chemical landscape within the divots. A purely diffusive environment limits access to ambient nutrients carried in the flow, and in tandem with locally-generated ciliary flows, corals rely on currents to flush carbon dioxide and other excrement away while bringing in nutrients and dissolved oxygen for growth (Kiel and Prakash 2022). Minimal flow also allows pH to be significantly higher in the divots compared to the surface. While the intention of the experiment was to expose coral to higher alkalinity conditions, it is possible that the chemical environment within the divots was too extreme. Additionally, one consequence of using the flumes to grow coral was that the tiles had to be cleaned by hand rather than co-reared with herbivores to control algal growth. Scraping algae out of the divots during cleaning was a delicate process in such a tight space while not harming coral. The algae in the divots could have served as additional competition for resources in an already resource-limited environment (Doropoulos et al. 2016).

Survivorship over the 130-day experiment, regardless of settlement location, increased by a factor of 2.5 to 2.9-fold on the 1% and 2% carbonate tiles compared to the tiles not receiving

any addition (**Figure 3**), however, growth had minimal variation with respect to chemistry (**Figure 4**). We initially hypothesized that any increase in survivorship would be a result of increased growth. Ocean acidification makes it difficult for calcifying organisms to build their carbonate skeletons, particularly during early stages of development, by raising the energetic demands for growing skeletons (Kurihara 2008, Albright et al. 2010, Waldbusser et al. 2015, Frieder et al. 2017). For corals, the first deposition of $CaCO_3$ for skeletal growth occurs during the first week or two after metamorphosis. The quicker this initial deposition occurs, the greater the success of the organism surviving to reproductive maturity (Kurihara 2008).

When planning for these experiments, we envisioned that AE tiles would elevate pH in the laminar boundary layer and corals would benefit from that environment while they were small enough to occupy that zone by growing faster. The observation that survivorship is improved on AE tiles without significantly faster growth suggests that corals benefit from the AE tile chemistry without augmenting their skeletal growth. It is possible that corals survived better because their energy was reallocated to other important processes rather than skeletal growth that were unaccounted for in the experiment such as tissue growth.

Corals may also benefit from tile chemistry through direct contact with the substrate, in addition to benefiting through the flow. This is evidenced by the enhanced survivorship on tiles that had the least effect on pH under flow – 2% carbonate addition tiles (**Figure 3**). Hence, carbonate and bicarbonate ions may leach from the substrate directly into coral tissues from the point contact under the corals, and the elevation of pH in the boundary layer may be less important.

Implications for Restoration Efforts

There is growing interest in the U.S., as well as around the world, to combine the use of built and natural infrastructure to help coastal communities become more resilient to extreme events and reduce the risk of coastal flooding through the creation of hybrid coastal resilience structures. To date, built infrastructure, including sea walls, levees, culverts, bulkheads, and other hardened structures, have dominated thinking about coastal protection (Spalding et al., 2014). However, there is an increasing interest in using natural habitats, including wetlands, dunes, barrier islands, sea grasses, coral and oyster reefs, and mangroves to reduce the risk of coastal flooding and erosion and provide other social and economic benefits (Sutton-Grier et al 2015). Many of the co-benefits associated with natural infrastructure are precisely what make coastal areas so valuable and what draws people to live and work in these oft-vulnerable regions. The coastal ecosystems that enhance resilience by providing protective services also contribute raw goods and materials, plant and animal habitat, water and air quality regulation, carbon sequestration, nutrient cycling, and opportunities for tourism, recreation, and education (Barbier et al., 2011).

One such hybrid approach is the deployment of an artificial reef base structure consisting of a submerged breakwater onto which reef-building corals are actively restored. Coral reefs are naturally formed, low-crested breakwaters that aid in wave energy dissipation and flood reduction and represent biodiversity hot spots that provide valuable ecological and economic benefits (Moberg and Folke 1999, Beck et al. 2018). Healthy coral reefs can attenuate wave energy by up to 97%, providing tremendous natural protection from coastal hazards (Ferrario et al. 2014). Considering this, hybrid reefs might best be thought of as opportunities to offer communities the immediate benefits of shoreline protection and the long-term benefits of restoring coral reefs, and important economic benefits and ecological services. In fulfillment of this vision, hybrid coral reef projects would become testbeds for testing new methods of coral restoration and increasing coral resiliency to climate change.

In summary, our results show that AE substrates can be an effective and scalable intervention method for improving early coral recruit survivorship in laboratory settings. These AE substrates could be potentially attached to artificial reef base structures in the ocean to hasten and facilitate the development of a natural coral reef biota on the structure. Although more work is needed to prove the benefits of AE substrates for coral reef restoration, and to bring hybrid coral reefs to reality, our promising results inspire optimism.

Materials and Methods

Tile Fabrication (Chemistry)

Three different chemical modifications to Portland limestone cement were tested in addition to unmodified cement with 0.4 water-to-cement ratio. The chemical modifications utilized were 1% sodium bicarbonate, 1% sodium carbonate, or 2% sodium carbonate by weight to cement. Chemical modifications and cement were dry-mixed using a spatula for 4 min to achieve homogeneity, followed by mixing with water for an additional 4 min. All mixtures with added chemicals showed minor reductions in workability from visual observations. Tiles (3 cm x 3 cm x 1 cm) were cast from these four types of AE cement – no additions, 1% bicarbonate, 1% carbonate, and 2% carbonate – referred to as "chemistries". Two different surface topographies were fabricated using 3D printed female molds – one where the surface of the tile contained no textural modifications (a "flat" tile), and one where the tile featured a 4 x 4 grid of circular, 3 mm-diameter, 3 mm deep divots spaced 5 mm from each other, centered on the tile (a "textured" tile; **Figure S1b**). Molds were filled with paste and placed on a vibration table to remove entrapped air, compacting the mix. The tiles were demolded 24 h after casting by drilling a hole in the bottom of the mold and applying compressed air. Subsequently, tiles were cured in a high relative humidity room (> 95% relative humidity) at 23 C for 28 d to ensure adequate hydration of cementitious materials.

After curing, tiles were transported from the University of Miami main campus (Coral Gables, FL) to the Rosenstiel School of Marine, Atmospheric, and Earth Science campus (Key Biscayne, FL). Tiles for diffusion experiments were stored in plastic bags until use. Tiles for advection and aging experiments were stored in a 38 L saltwater tank with a bubbler to ensure constant mixing. Tiles for biological experiments were further conditioned for 30 d in running seawater with live rock for colonization by crustose coralline algae (CCA) and biofilms that would provide attractive cues for *O. faveolata* larvae to encourage settlement (Ritson-Williams et al. 2014, Quinlan et al. 2023).

To characterize the chemical effect of the four different AE cements, pH was measured using UNISENSE microelectrodes (pH-N; 1.1 mm x 40 mm needle electrode with external reference electrodes, **Figure S2a**). To estimate the diffusive potential of the AE tiles and confirm that they change pH, one randomly selected flat tile of each of the four chemistries was measured over a 24 h period to quantify the diffusive capacity of the tiles to change pH in the water column. For measurements, the tile was transferred to 1000 mL of water. Microelectrodes were positioned at the surface and 2 mm above the surface of the tile. Sensors sampled at a frequency of 1 Hz for 24 hrs.

Simulating the Hydrodynamic Landscape (Flow + Chemistry)

The hydrodynamic and chemical landscape quantifications in this experiment required the design of a flume that could: (1) achieve flows representative of natural coral reef environments (Shashar et al. 1996, Enochs et al. 2023), (2) be used in particle image velocimetry experiments to quantify flow fields, and (3) be used in chemistry experiments to easily observe the effects of AE tiles without needing to make changes to the bulk water chemistry. For reasons

(2) and (3), we utilize two configurations of a modular flume – a flow-through configuration and a recirculating configuration (Ruszczyk et al. preprint). Both configurations feature the same experimental chamber where measurements are carried out. The flow-through configuration is open-ended, allowing for a constant flow of water through the experimental chamber and the recirculating configuration is fully enclosed, allowing for easy PIV measurements. A brief description of the modular flume, configurations, and flow conditions is provided here, with a more detailed description of the design, testing, and validation in (Ruszczyk et al. preprint)

The experimental chamber in both configurations is comprised of a 30 cm x 10 cm x 14.5 cm transparent acrylic tank with inlet and outlet points made from 3 in, schedule-40 PVC pipe (**Figure 1b**). A 5 cm flow straightener with a hexagonal grid (hexagon circumscribed diameter = 1 cm) is mounted in the upstream direction of the experimental chamber. A 29 cm x 9.8 cm x 1.9 cm plate made of ¾ in PVC was made to hold a 1 x 3 configuration of three tiles along the length of the experimental chamber. Three indentations of dimensions 3.2 cm x 3.2 cm x 1.3 cm were made in the center of the plate, separated by 4.5 cm centered in the middle, to recess tiles such that the surface of the tiles was exposed to flow. The top of the tile plate rested flush with the bottom of the PVC inlet and outlet pipes. In the recirculating and flow-through flume configurations, the experimental chamber was filled such that the surface of the water was flush with the top of the inlet and outlet PVC, resulting in a volume of 2.28 L in the acrylic chamber.

To create a flow-through configuration (**Figure 1c**) where water is constantly turned over, the flumes were connected to a saltwater tap that supplied seawater filtered from the neighboring Biscayne Bay. Four flow-through flumes were installed on one tap line, branching off from a ¾ in PVC mainline. A ball valve at the top of each individual flume's line allowed for volumetric flow control over each flume placed on the line. After the ball valve, the water flowed through a 1.9-19 L min^{-1} (0.5-5 gal min^{-1}) clear in-line flow meter (Omega Engineering) to observe the incoming volumetric flow rate. The water then travelled through a 0.60 m section of 3 in PVC pipe before reaching the inlet of the experimental chamber. The outlet flow was controlled by adjusting a 3 in PVC elbow joint fixed to the outlet of the experimental chamber, and was set such that surface of the water was flush with the top of the inlet and outlet pipes of the experimental chamber.

The recirculating configuration was made by connecting the inlet and outlet pipes of the experimental chamber via a 3 in PVC pipe. An inverted tee joint at the back of the track allowed for a DC motor (Almencla RC Jet Boar Motor Engine Propellor) mounted to PVC pipe to be inserted. The motor was powered by an external power supply to achieve various flow rates. A laminar flow in the experimental chamber with a bulk flow speed of 1.20 cm s^{-1} was generated (Reynolds number = 3550) in all flow-based experiments, matching reef-like conditions (Hata et al. 2017) (**Figure 1d**).

To estimate the effect of AE tiles in flow conditions, the pH at the tile surface for the four different chemistries was measured in a flow-through flume. One tile of each chemistry was transferred to a flow-through flume and placed in the upstream tile position. Sampling took place via UNISENSE pH microelectrodes positioned at the surface of the tile and approximately 1 cm above the surface of the tile (**Figure S2**). Microelectrodes measured the pH at 1 Hz for 6 h to generate a time series of the influence of chemistries on the local pH at and above the tile surface.

To estimate the longevity of the AE tiles' enhancement effect, 12 flat cement tiles – three of each chemistry – was measured for 84 d. Tiles were stored in a 3 x 4 grid in a surplus flow-through flume filled with seawater and a bubbler to ensure mixing while experiments were not occurring – a storage flume. The storage flume was connected to the experimental flume such that when experiments occurred, all tiles were exposed to experimental flow conditions. The pH was measured at the surface of the tile to capture changes within the laminar boundary layer and was measured 3.26 $\pm$ 0.09 mm above the surface of the tile to capture changes above the

laminar boundary layer and within the laminar boundary layer. AE tiles were measured in the upstream slot of the tile-holder for 90 min in a flow-through flume with a volumetric flow rate of 0.05 L s^{-1} (1.20 $\pm$ 0.3 cm s^{-1}) for one of each of the four different chemistries daily for 30 d. After the first 30 d, experiments were performed every other day. The experimental tiles on a given day were randomly selected with no replacements until all 12 tiles had been recorded. After all tiles were measured, the tile position in the storage tank was shuffled, and all tiles were allowed to be selected for experiments again. This ensured a sample size of n = 3 for each of the four different chemistries.

Microelectrodes and reference electrodes were held in the experimental flume via dual micromanipulators (UNISENSE). Microelectrodes were positioned at the center of the downstream edge of the tile (**Figure S2b, c, d**) and the reference electrodes and temperature sensor were placed downstream in the experimental flume to not disturb the flow above the experimental tile. At the beginning of each day, flow was turned on to the flow-through system for the storage flume and the experimental flumes. Microelectrodes were positioned in the tank and allowed to acclimate for up to 30 min or until they provided a steady pH reading of ambient fluid for 10 min. After this acclimation period, a tile was added to the upstream tile position in the tile plate, and microelectrodes were deployed to record data. Microelectrodes ran for 90 min. After this time, the tile was removed, and the microelectrodes were allowed to reacclimate to ambient water for 10 min before the next tile was added. This was repeated such that one tile of each chemistry type was measured per day. Microelectrodes were recalibrated with buffer solutions of standard pH values once per week.

The effect of topography on chemistry was tested by concurrently sampling the pH of textured tiles on the surface of the tile and within a divot on the same tile in a flow-through flume (**Figure S2e**). The first microelectrode was positioned to measure at the bottom of the divot, and the second was positioned within 10 mm of the divot such that it was touching the surface of the tile. Microelectrode positions were measured by photographing the profile and the top-down angle with known reference measurements. One tile of each of the four different chemistries was measured three times over the course of three days for 90 min each day to account for any daily variation in the tile.

The hydrodynamic landscape over flat and textured tiles was quantified in the recirculating flume using 2-dimensional planar particle image velocimetry (PIV). To record the flow over different tile topographies, a tile was placed in the upstream position of a tile-holder. The recirculating flume was seeded with 60 µm diameter polyamide particles (LaVision) and illuminated with a 1350 lumen LED illumination unit (LaVision) mounted above the tank creating a light sheet (**Figure S3**). The thickness of the light sheet was reduced to 1 cm by manually blocking the light entering the tank. The flow was set to a bulk flow velocity of 1.20 cm s^{-1} using pre-established settings. Once the flow was steady, a 10 s video of the flow above the tile was recorded. Recording took place using an Imager CS2 5 Camera mounted with a L 60 mm focal length lens (F/2.8, 2:1 macro, LaVision) at 40 Hz. Flow quantification over tile topographies took place over an 8 cm x 6 cm window parallel to flow bisecting the tile, resulting in a resolution of approximately 320 px cm^{-1}.

Orbicella faveolata *Settlement and Growth on Tiles (Biology + Flow + Chemistry)*

To test how coral recruits respond to AE cement tiles, *O. faveolata* larvae were settled and grown on AE tiles. Not all chemistries, or combinations of chemistry and topography type could be tested due to spatial limitations. We excluded bicarbonate additions for the biology experiment because bicarbonate is not as effective at uptaking H^+ as carbonate, thus maximizing the chance of observing any differences in growth related to chemistry. The three chemistry treatments were thus no additions, 1% carbonate additions, and 2% carbonate additions. Each chemistry included a set of flat tiles, and the no additions and 1% carbonate additions chemistries

included a set of textured tiles, resulting in 5 different combinations of chemistry and topography in the biological subset of tiles.

Orbicella faveolata eggs and sperm were collected at Horseshoe Reef (25.1399° N, 80.2946° W) in Key Largo, FL, during a natural spawning event on August 7-8, 2023, and fertilized in-vitro. The larvae were transferred to three polystyrene settlement bins at a density of approximately 300 per bin. Each bin contained a random assortment of 25 treatment tiles, and 5 mL of crushed *Hydrolithon boergesenii* (Ritson-Williams et al. 2014) in UV-sterilized, 1 µm filtered seawater. Settlement bins were kept in a temperature-controlled incubation room at 27 °C and daily 75% water changes were conducted while the larvae settled on the cement tiles over 5 weeks. Larvae were characterized as settled, upon achieving full metamorphosis on the cement tiles, distinguished by a more circular, squat morphology in contrast to the elongated shape of freeform larvae. *S*ettlers were counted and spatially mapped across all experimental tiles using a dissection microscope (**Figure S4a**). Tiles were labeled using waterproof paper tag affixed on the side of the tile using CorAffix gel coral glue. The three tiles of each tile type of the biological subset exhibiting the highest settlement densities on the upper surface were selected for grow out in the flow-through flumes, totaling 180 coral recruits across 15 tiles.

Orbicella faveolata were inoculated with symbionts three times per week for 10 weeks. Inoculation occurred 5 weeks prior to relocation in flumes and the first 5 weeks residing in the flumes. *Orbicella faveolata* were inoculated with *Durusdinium* algal culture isolated from Key Largo, FL, in the early 2000s. *Durusdinium* cultures were maintained in an incubator at 27 °C in f/2 media with a 14:10 light:dark photocycle under 40 µE light at a density of 10^6 cells mL^{-1}. To inoculate *O. faveolata*, tiles were transferred from their respective tanks to polystyrene bins containing 3,000 cells mL^{-1} of *Durusdinium* algal culture for 6 hrs. Inoculation continued until each polyp on the tiles exhibited color indicative of symbiont saturation. During the inoculation period, tiles received 30 µmol s^1 m^{-2} of photosynthetically available radiation (PAR) on a 12:12, light:dark photocycle.

Tile position within the flume was randomized 3 times per week to reduce possible downstream effects from the AE tiles. Tile groups were assigned to different flumes twice per week to ensure randomness across flumes. Twice per week, tiles were relocated to 19 L tanks in a 28 °C, temperature-controlled bath for 45 min, and fed with Golden Pearls coral food. In traditional coral tanks, herbivores are co-reared with corals to control algae growth. Herbivores were not used in this experiment due to unsteadiness in flows around the additional organisms, and the threat that they would maneuver outside of the experimental chamber in the flow-through flumes. Instead of relying on herbivores to control algae growth, tiles were manually cleaned twice per week using a 25-gauge needle under a dissection microscope to ensure all algae were removed from the surface of the tile.

To consistently identify corals throughout the experiment, settlement maps were made by taking an areal image of the full tile and updated weekly. Each recruit was assigned a unique ID, comprised of its tile number and a letter. Settlement maps provided confidence in individual coral measurement for the entirety of the experiment between multiple researchers collecting data.

Coral measurements occurred weekly. Survivorship was visually assessed by observing polyp activity during cleaning and measurement periods. For areal measurements, tiles were transferred to a 100 mL dish and imaged under a dissecting microscope. Images included a ruler in the background for scaling. For vertical growth measurements, corals were transferred to the recirculating flume with no flow present and imaged in a vertical profile using the PIV camera. Corals were located on the tile by mounting a calibration wand to a micromanipulator positioned above the tank. Referencing the settlement maps, the calibration wand was moved to the approximate position of the coral. The image was refined by adjusting the lens on the camera until the coral was in focus. The calibration wand was then physically adjusted to be in focus with

the coral, ensuring that a known reference measurement was present in each image. As the image library was generated, old photos were cross-referenced to ensure consistent camera positioning throughout the experiment (**Figure S4c-d**).

Data processing

Chemistry data for tiles was processed using a custom written MATLAB code. Chemical data collected from microelectrodes was first transformed from the logarithmic pH measurements to linear $[H^+]$ measurements by

$$[H^+] = 10^{-pH} \tag{3}$$

allowing for processing and analysis using linear techniques. To account for slight differences in calibration between microelectrodes and daily differences in ambient pH in experiments, the change in $[H^+]$ (ΔH^+) is used, rather than absolute $[H^+]$ measurements. To calculate ΔH^+, the time series data was transformed such that the average $[H^+]$ in the 10 min calibration period of each time series is equal to zero. To account for sensor drift in the microelectrodes, data was detrended using a natural logarithmic function fitted to the calibration period of the data.

Flow data for tiles was processed in DaVis 11.0.0.196 software (LaVision). For PIV over tile topographies, a mask was applied to the bottom of the tank to exclude any areas where the tile may have protruded above the tile-holder. PIV was performed using a bicubic interpolation to interpolate vectors, 5 x 5 denoising, a symmetrical shift correction mode. Pixels were interpolated using a spline interpolation mode with a window interrogation size of 16 px x 16 px, a direct correlation algorithm was used between frames, and cell size weighted as a round cell. These parameters resulted in an average correlation value of 1.00 px.

Orbicella faveolata data was first scanned to exclude any chimeras (n=5) – instances of two adjacent settlers fusing to form one large entity – from the analysis. Data was analyzed using three response variables: settlement preference, survivorship, and growth. Settlement preference was assessed by counting the total number of *O. faveolata* settlers per tile, parsed by settlement location (i.e., on the surface or in a divot). Two different measures of survivorship were calculated and analyzed. Total survivorship with respect to the tile was calculated each week as the ratio of all surviving *O. faveolata* on a given tile to the initial number of settlers on that tile, regardless of settlement location. Survivorship was partitioned for textured tiles into the ratio of surviving *O. faveolata* settlers on flat surface versus in divots, relative to the initial number of settlers in those locations – location survivorship. For flat tiles, only survivorship of flat surface settlers was calculated, as there were no divots present.

Polyp surface area was calculated by analyzing images in ImageJ software (version 1.54g). The polyps in photos were outlined twice with the freehand tool and the area was calculated and measured twice. The radius of the coral, *r*, was estimated from this area, assuming the fitted shape was a circle. Vertical measurements were analyzed in DaVis 11.0.0.196 software. Vertical height was measured from the surface of the tile to the visible skeletal height, identifiable by a change in contrast in the image. Volumetric growth was calculated using the areal and profile images. Coral volume (mm^3) was modelled as a cylinder, using the radius of the fitted circle calculated in areal measurements and the skeletal height of the coral as

$$V = \pi r^2 h \tag{4}$$

where *r* is the radius (mm) of the areal measurements and *h* is the skeletal height (mm) of the coral (**Figure 1b**).

Statistical Analysis

Statistical analysis for chemical characterization of tiles was performed on ΔH^+ to allow for analysis using linear techniques. Results reporting chemical differences are presented as ΔpH

values, for ease of understanding. The influence of tiles on local pH via diffusion and advection was assessed using an ANOVA on one 6 h time series for each chemistry type for each flow condition. Aging data was modelled using linear regressions fitted to the average daily ΔH^+ at the surface and above the surface for each chemistry. The effect of topography on chemistry was assessed using an ANOVA on one 1.5 h time series for each chemistry.

Flows over surface topographies were compared via velocity and vorticity measurements at similar spatial coordinates. The data was checked for outliers resulting from PIV analysis, and outliers were removed from the dataset.

Orbicella faveolata data was analyzed with respect to tile. Settlement preference was analyzed by the initial number of settlers (0 d) using a factorial ANOVA, with chemistry and topography as factors. *Orbicella faveolata* total survivorship was analyzed at the conclusion of the experiment (139 d) using a factorial ANOVA with chemistry and topography as factors. On the textured tiles, where larvae had the option of settling in different settlement locations (i.e., on the surface or within a divot), the percentage of settlers based on location (survivorship with respect to location) for the textured tiles was calculated as the amount settled in each location per tile (i.e., on the exposed surface or in a divot) and was analyzed via student's t-test with settlement location as a factor.

To remove any selective bias in growth data from smaller corals dying, growth data was filtered to only include colonies which survived the duration of the experiment. Growth analysis only included measurements for corals grown on the flat surfaces of tiles, as vertical measurements could not be obtained for corals which settled in the divots of textured tiles. Growth data (surface area, skeletal height, and volume) was analyzed using generalized linear models (GLMs). GLMs analyzed growth data with respect to age (days in flume) and a factorial design of chemistry and topography using an inverse function linked to a gamma distribution. AIC values of each model were compared within dependent variables to determine the best fitted model.

Statistical analysis was performed in JMP 16.0 (SAS Institute 2023) and R 4.4.1 (R Core Team 2022). Assumptions for normality and heteroscedasticity were verified on all the data, allowing for parametric ANOVAs and Tukey's HSD using the DHARMa package (Hartig et al. 2022) in R. All data is presented as mean $\pm$ standard error unless otherwise stated.

Acknowledgments

The authors would like to acknowledge all members of the X-REEFs team (Reef Engineering to Enhance Future Structures project, funded by the Defence Advanced Research Projects Agency) for their support. Additionally, the authors thank Dr. Sanchit Mehta and the students in the SUSTAIN laboratory at the University of Miami, Johnnia Xia, Owen Brown and Patrick M. Kiel in the Prakash Lab and Cedric M. Guigand (Rosenstiel School Maker Shop) for flume development, design, and initial testing, Clara Haughey-Gramazio in the Langdon Lab for coral assistance, Dr. Mary Alice Coffroth for *Durusdinium* cultures (University at Buffalo), as well as all members of the Suraneni, Baker, Langdon, and Prakash Labs for useful discussions. The authors also thank Dr. Douglas Neal from LaVision Inc, for installation and support of the PIV system. V.N.P. would like to acknowledge start-up funding support from the University of Miami.

This material is based upon work supported by the Defense Advanced Research Projects Agency under the Reefense Program, BAA HR001121S0012. The views, opinions and/or findings expressed are those of the author and should not be interpreted as representing the official views or policies of the Department of Defense or the U.S. Government.

References

Albright, R., L. Caldeira, J. Hosfelt, L. Kwiatkowski, J. K. Maclaren, B. M. Mason, Y. Nebuchina, A. Ninokawa, J. Pongratz, K. L. Ricke, T. Rivlin, K. Schneider, M. Sesboüe, K. Shamberger, J. Silverman, K. Wolfe, K. Zhu, and K. Caldeira. 2016. Reversal of ocean acidification enhances net coral reef calcification. Nature **531**:362-365.

Albright, R., B. Mason, M. Miller, and C. Langdon. 2010. Ocean acidification compromises recruitment success of the threatened Caribbean coral. Proceedings of the National Academy of Sciences of the United States of America **107**:20400-20404.

Barbier, E.B., Hacker, S.D., Kennedy, C., Koch, E.W., Stier, A.C., Silliman, B.R., 2011. The value of estuarine and coastal ecosystem services. Ecol. Monogr. 81, 169–193.

Beck, M. W., I. J. Losada, P. Menéndez, B. G. Reguero, P. Díaz-Simal, and F. Fernández. 2018. The global flood protection savings provided by coral reefs. Nature Communications **9**.

Doropoulos, C., G. Roff, Y. M. Bozec, M. Zupan, J. Werminghausen, and P. J. Mumby. 2016. Characterizing the ecological trade-offs throughout the early ontogeny of coral recruitment. Ecological Monographs **86**:20-44.

Enochs, I. C., M. S. Studivan, G. Kolodziej, C. Foord, I. Basden, A. Boyd, N. Formel, A. Kirkland, E. Rubin, M. Jankulak, I. Smith, C. R. Kelble, and D. P. Manzello. 2023. Coral persistence despite marginal conditions in the Port of Miami. Scientific Reports **13**.

Ferrario, F., M. W. Beck, C. D. Storlazzi, F. Micheli, C. C. Shepard, and L. Airoldi. 2014. The effectiveness of coral reefs for coastal hazard risk reduction and adaptation. Nature Communications **5**.

Frieder, C. A., S. L. Applebaum, T. C. F. Pan, D. Hedgecock, and D. T. Manahan. 2017. Metabolic cost of calcification in bivalve larvae under experimental ocean acidification. Ices Journal of Marine Science **74**:941-954.

Guannel, G., K. Arkema, P. Ruggiero, and G. Verutes. 2016. The power of three: Coral reefs, seagrasses and mangroves protect coastal regions and increase their resilience. PLoS ONE **11**.

Hartig, F., L. Lohse, and M. de Souza Leite. 2022. DHARMa: Residual diagnostics for hierarchical (Multi-Level/Mixed) regression models.

Hata, T., J. S. Madin, V. R. Cumbo, M. Denny, J. Figueiredo, S. Harii, C. J. Thomas, and A. H. Baird. 2017. Coral larvae are poor swimmers and require fine-scale reef structure to settle. Scientific Reports **7**.

Herfort, L., B. Thake, and I. Taubner. 2008. Bicarbonate stimulation of calcification and photosynthesis in two hermatypic corals. Journal of Phycology **44**:91-98.

Hughes, T. P., A. H. Baird, E. A. Dinsdale, N. A. Moltschaniwskyj, M. S. Pratchett, J. E. Tanner, and B. L. Willis. 1999. Patterns of recruitment and abundance of corals along the Great Barrier Reef. Nature **397**:59-63.

Humanes, A., and C. Bastidas. 2015. In situ settlement rates and early survivorship of hard corals: a good year for a Caribbean reef. Marine Ecology Progress Series **539**:139-151.

Kiel, P. M., and V. N. Prakash. 2022. Coral physiology: Going with the ciliary flow. Current Biology **32**:R998-+.

Kurihara, H. 2008. Effects of CO2-driven ocean acidification on the early developmental stages of invertebrates. Marine Ecology Progress Series **373**:275-284.

Langdon, C., T. Takahashi, C. Sweeney, D. Chipman, J. Goddard, F. Marubini, H. Aceves, H. Barnett, and M. J. Atkinson. 2000. Effect of calcium carbonate saturation state on the calcification rate of an experimental coral reef. Global Biogeochemical Cycles **14**:639-654.

Levenstein, M. A., D. J. Gysbers, K. L. Marhaver, S. Kattom, L. Tichy, Z. Quinlan, H. M. Tholen, L. W. Kelly, M. J. A. Vermeij, A. J. W. Johnson, and G. Juarez. 2022. Millimeter-scale topography facilitates coral larvael settlement in wave-driven oscillatory flow. PLoS ONE **17**:e0274088.

Moberg, F., and C. Folke. 1999. Ecological goods and services of coral reef ecosystems. Ecological Economics **29**:215-233.

Munson, B. R., T. H. Okiishi, W. W. Huebsch, and A. P. Rothmayer. 2013. Fundamentals of Fluid Mechanics. 7 edition. Wiley.

Quinlan, Z. A., M. J. Bennett, M. G. I. Arts, M. Levenstein, D. Flores, H. M. Tholen, L. Tichy, G. Juarez, A. F. Haas, V. F. Chamberland, K. R. W. Latijnhouwers, M. J. A. Vermeij, A. W. Johnson, K. L. Marhaver, and L. W. Kelly. 2023. Coral larval settlement induction using tissue-associated and exuded coralline algae metabolites and the identification of putative chemical cues. Proc Biol Sci **290**:20231476.

Ritson-Williams, R., S. N. Arnold, V. J. Paul, and R. S. Steneck. 2014. Larval settlement preferences of Acropora palmata and Montastraea faveolata in response to diverse red algae. Coral Reefs **33**:59-66.

Ruszczyk, M., P. M. Kiel, S. Chandragiri, C. M. Guigand, J. Xia, O. Brown, B. K. Haus, A. C. Baker, M. W. Miller, P. Suraneni, C. Langdon, and V. N. Prakash. preprint. FlumeX: A modular flume design for laboratory-based marine fluid-substrate studies.

Shashar, N., S. Kinane, P. L. Jokiel, and M. R. Patterson. 1996. Hydromechanical boundary layers over a coral reef. Journal of Experimental Marine Biology and Ecology **199**:17-28.

Souter, D., S. Planes, J. Wicquart, M. Logan, D. Obura, and F. Staub. 2021. Status of Coral Reefs of the World: 2020 executive summary.

Spalding, M.D., Ruffo, S., Lacambra, C., Meliane, I., Hale, L.Z., Shepard, C.C., Beck, M.W., 2014. The role of ecosystems in coastal protection: adapting to climate change and coastal hazards. Ocean Coast. Manage. 90, 50–57.

Sutton-Grier, A. E., K. Wowk and H. Bamford (2015). "Future of our coasts: The potential for natural and hybrid infrastructure to enhance the resilience of our coastal communities, economies and ecosystems." Environmental Science & Policy **51**: 137-148.

Vardi, T., W. C. Hoot, J. Levy, E. Shaver, R. S. Winters, A. T. Banaszak, I. B. Baums, V. Chamberland, N. Cook, D. Gulko, M. Y. Hein, L. Kaufman, M. Loewe, P. Lundgren, C. Lustic, P. MacGowan, M. V. Matz, M. McGonigle, I. McLeod, J. Moore, T. Moore, S. Pivard, F. J. Pollock, B. Rinkevich, D. J. Suggett, S. Suleiman, T. S. Viehman, T. Villalobos, V. M. Weis, C. Wolke, and P. H. MontoyaMaya. 2021. Six priorities to advance the science and practice of coral reef restoration worldwide. Restoration Ecology **29**.

Waldbusser, G. G., B. Hales, C. J. Langdon, B. A. Haley, P. Schrader, E. L. Brunner, M. W. Gray, C. A. Miller, and I. Gimenez. 2015. Saturation-state sensitivity of marine bivalve larvae to ocean acidification. Nature Climate Change **5**:273-280.

Whalan, S., M. A. Abdul Wahab, S. Sprungala, A. J. Poole, and R. de Nys. 2015. Larval Settlement: The Role of Surface Topography for Sessile Coral Reef Invertebrates. PLoS ONE **10**.

Wilson, J., and P. Harrison. 2005. Post-settlement mortality and growth of newly settled reef corals in a subtropical environment. Coral Reefs **24**:418-421.

Figures and Tables

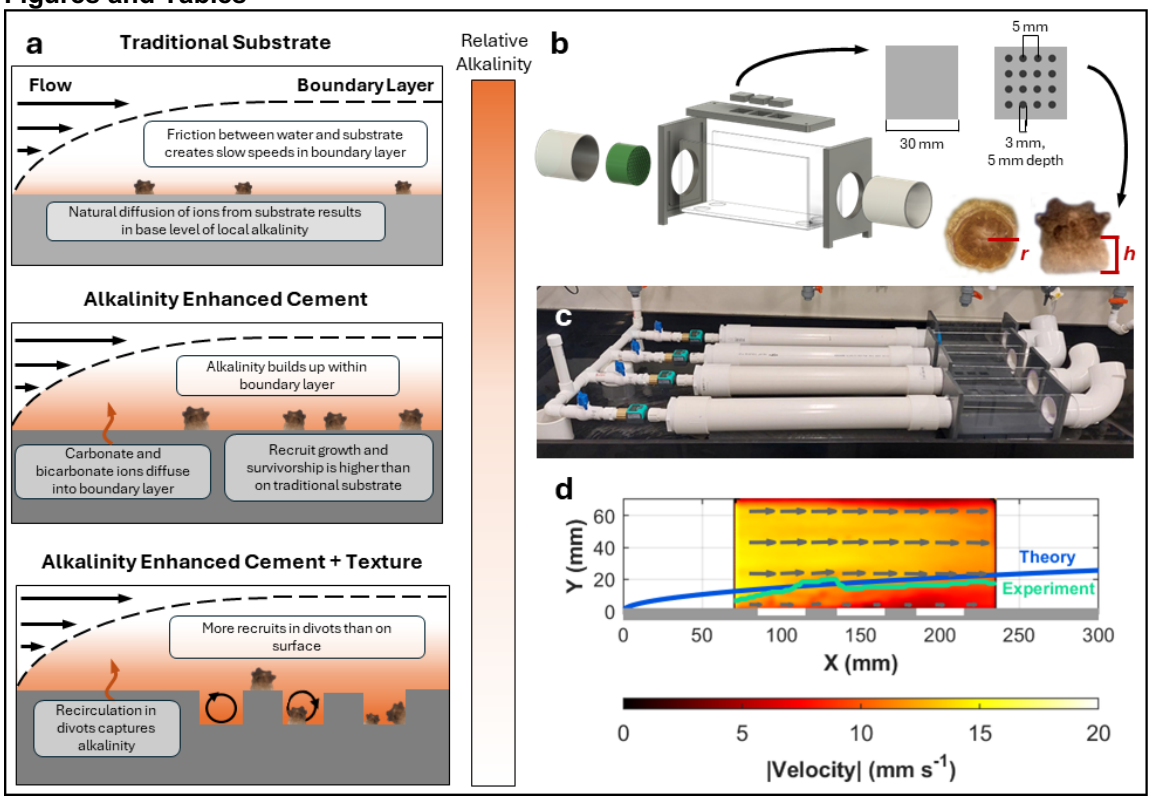

Figure 1. Local alkalinity enhancement concept and experiments. (a) Top panel: Coral recruits (< 1 cm in height) grow within the laminar boundary layer of a substrate, where the local flow velocity is slower than the bulk flow above. Slower velocities inside the laminar boundary layer allow for ions that diffuse from the substrate to stay near the surface for longer times. Middle panel: Alkalinity enhanced substrates leach/release carbonate and/or bicarbonate ions into the water column, resulting in a higher alkalinity environment that corals can take advantage of, resulting in more growth and greater survivorship. Bottom panel: By modifying the topography of the substrate, it is possible to create a dynamic landscape with regions of even greater local alkalinity which may further enhance coral growth and survivorship. (b) Experimental viewing chamber design and flume components: Each chamber holds three cement tiles that are either flat or textured (with surface divots). *Orbicella faveolata* recruits grow on the surface of the cement tiles. Their radius, *r*, and skeletal height, *h*, are used to determine growth measurements. (c) Four flow-through flumes connect to one inlet line allowing for multiple experimental flumes. (d) Quantification of fluid flow in the flume viewing chamber where the tiles sit. The experimentally measured laminar boundary layer (green) and the theoretical boundary layer (blue) are included.

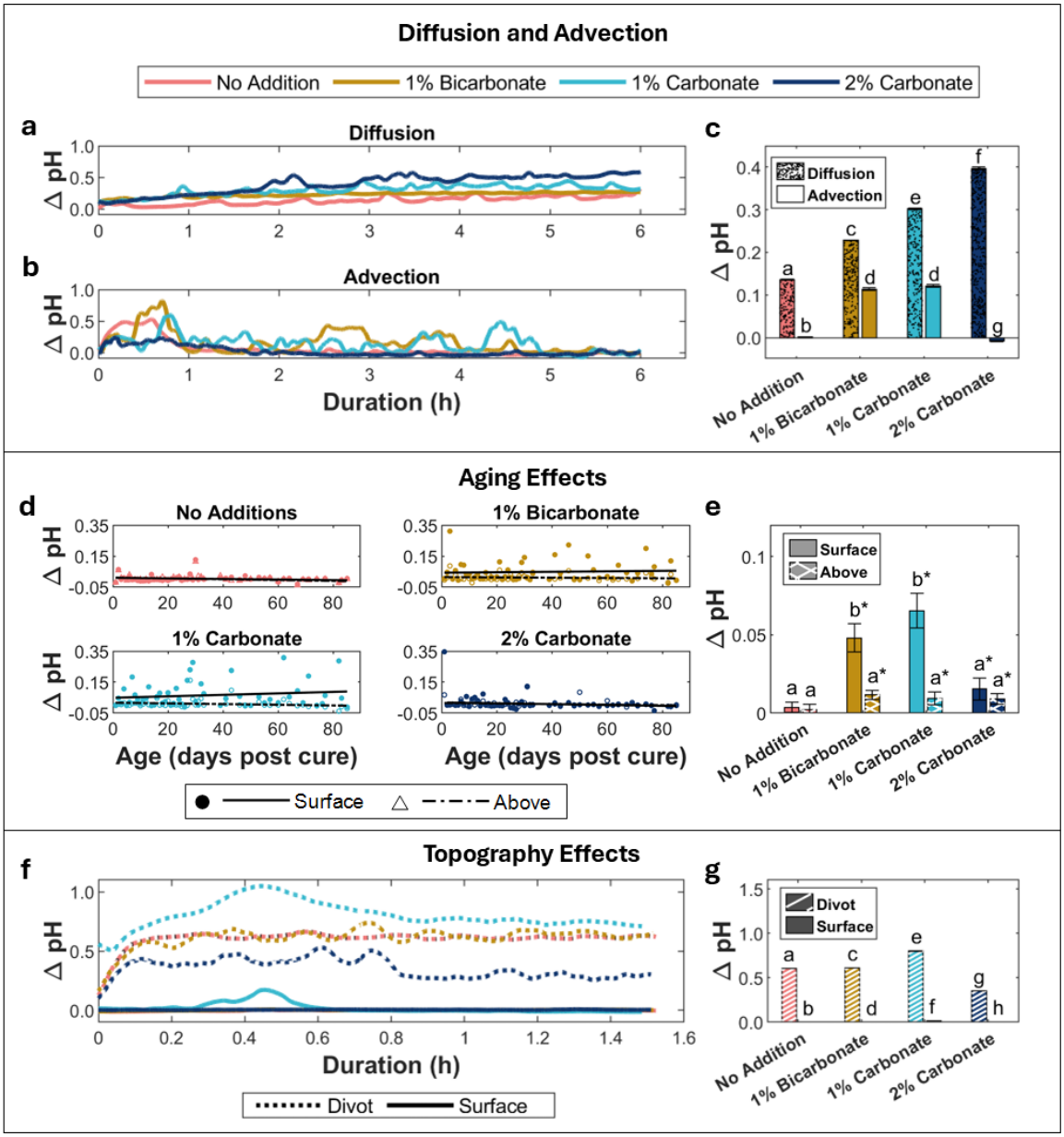

Figure 2. Physicochemical characteristics of AE tiles. (a) The first 6 h of a 24 h diffusion time series for flat tiles. (b) The first 6 h of a 24 h advection time series for flat tiles. (c) The average ΔpH from hour 1-6, after the tile reaches equilibrium with the environment. (d) Linear regressions fitted to ΔpH for tiles with no additions, 1% bicarbonate additions, 1% carbonate additions, and 2% carbonate additions, at the surface and 3.26 ± 0.09 mm above the surface of the tile to capture changes on the surface of the tile and within the laminar boundary layer in flow conditions. (e) Average ΔpH at and above the boundary layer of the four different chemistries throughout the 84 d aging experiment. Asterisks indicate average value greater than 0. (f) The first 90 min of advective time series on textured tiles measured at the surface of the tile and within a divot on a textured tile. (g) The average ΔpH over the duration of the advective time series for textured tiles. Throughout, different letters indicate statistically different data.

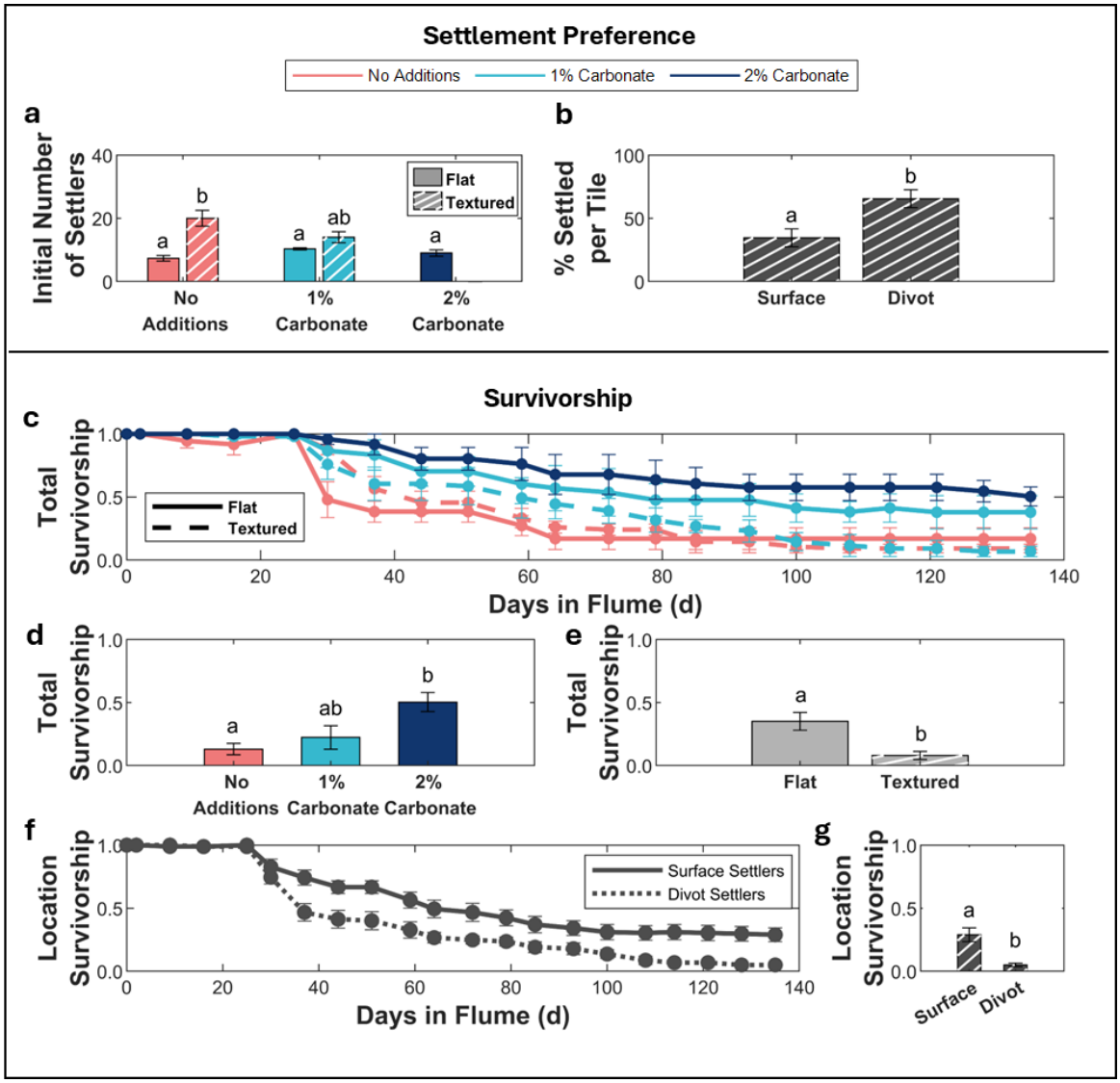

Figure 3: *Orbicella faveolata* settlement and survivorship. (a) The initial number of *O. faveolata* settlers on all five tile types tested. (b) The percentage of settlers based on location within the textured tiles. (c) Survivorship curves for the three different chemistries and the two different surface topographies. (d) Average total tile survivorship across all tiles (n = 15), regardless of settlement location, at the end of data collection with respect to chemistry. (e) Average total survivorship across all tiles (n = 15), regardless of settlement location, at the end of data collection with respect to topography. (f) Location survivorship curves for surface and divot settlers on textured tiles only (n = 6). (g) Average location survivorship with respect to settlement location at the end of data collection on textured tiles only (n = 6). Throughout, different letters indicate statistically different data.

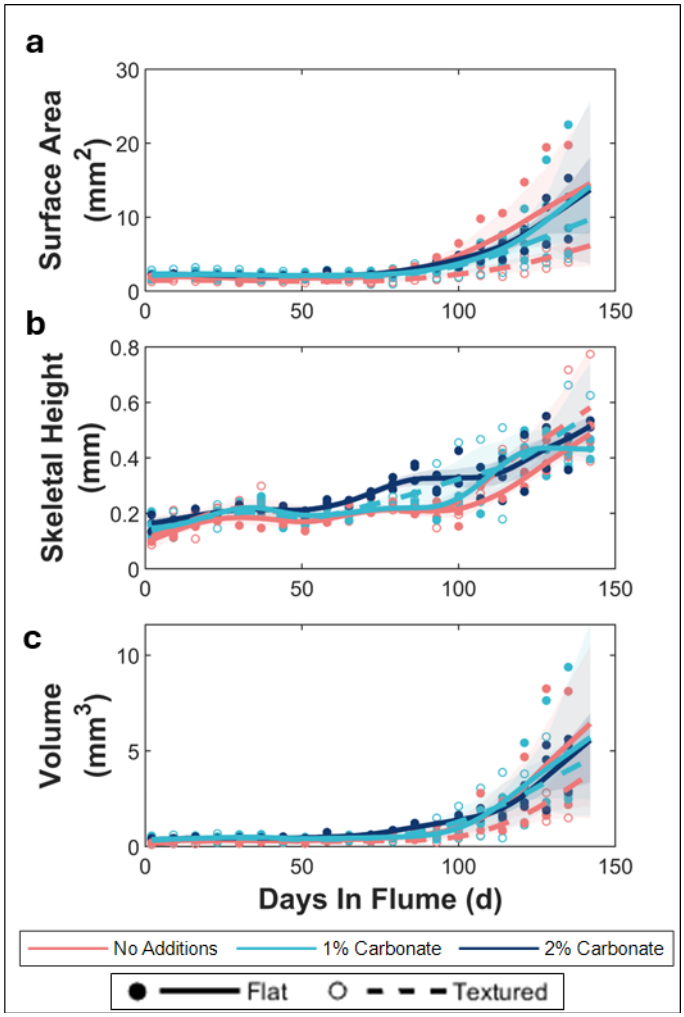

Figure 4: *Orbicella faveolata* growth. Spline-fitted curves and 95% confidence intervals for (a) surface area, (b) skeletal height, and (c) volume of *O. faveolata* settled on the surface of cement tiles. Data has been filtered to only include *O. faveolata* which survived until the end of the data collection period. Chemistry and topography are significant effects in GLMs run on the data.

Table 1: GLM Effect tests. Effect tests for significant factors in the best-fit GLM. The best fit GLMs for predicting surface area and volume were dependent on chemistry, topography, and an interactive effect of chemistry and topography, and the best fit GLM for predicting vertical height was dependent only on chemistry and topography (**Supplementary Table S5**).

		Surface Area	Vertical Height	Volume
Days in Flume	**DF(x,y)**	(1, 233)	(1, 249)	(1, 232)
	F	619.03	743.31	858.49
	p	<0.0001	<0.0001	<0.0001
Chemistry	**DF(x,y)**	(2, 231)	(2, 247)	(2, 230)
	F	5.33	8.34	3.3
	p	<0.01	<0.001	0.04
Topography	**DF(x,y)**	(1, 230)	(1, 246)	(1, 229)
	F	29.89	10.50	5.02
	p	<0.0001	<0.01	0.03
Interactive Effect	**DF(x,y)**	(1, 229)	NA	(1, 228)
	F	25.79	NA	7.97
	p	<0.0001	NA	<0.01